Applied Catalysis B: Environmental 110 (2011) 126–132

Contents lists available at SciVerse ScienceDirect

Applied Catalysis B: Environmental

journal homepage: www.elsevier.com/locate/apcatb

Photocatalytic bleaching of aqueous malachite green solutions by UV-A and blue-light-illuminated TiO_2 spherical nanoparticles modified with tungstophosphoric acid

J.A. Rengifo-Herrera *, M.N. Blanco, L.R. Pizzio *

Centro de Investigación y Desarrollo en Ciencias Aplicadas "Dr. J.J. Ronco" (CINDECA), Calle 47 N 257, Departamento de Química, Facultad de Ciencias Exactas, UNLP-CCT La Plata, CONICET, 47 No. 257, 1900 La Plata, Buenos Aires, Argentina

ARTICLE INFO

Article history:
Received 16 June 2011
Received in revised form 19 August 2011
Accepted 25 August 2011
Available online 1 September 2011

Keywords:
Heterogeneous TiO_2 photocatalysis
Tungstophosphoric acid
Malachite green
Visible light responsive TiO_2

ABSTRACT

Visible-light-responsive spherical TiO_2 particles were prepared by the sol–gel method by adding urea as pore-forming agent and tungstophosphoric acid (TPA) in different ratios (20% and 30% w/w) and by annealing at 500 °C for 2 h. Visible light absorption is probably due to WO_x formation (i.e. WO_3) resulting from the partial degradation of TPA and evidenced by XPS spectra. Besides, ^{31}P NMR and XPS results showed evidence about the existence of mostly unaltered TPA within TiO_2 nanoparticles and on their surface, together with lacunar or dimeric species. TPA addition not only affected the optical properties of materials but also produced a strong decrease of their point of zero charge (pH_{pzc}). Results obtained under UV-A irradiation revealed that aqueous malachite green (MG) solutions were efficiently bleached through the oxidative process of *N*-demethylation being the TiO_2 powder containing 30% (w/w) of TPA (TiO_2–TPA–30%) (100% of bleaching in 60 min) the most active even than Degussa P-25 (80% of MG bleaching in 60 min). On the other hand, when blue-light irradiation was used, TiO_2–TPA–30% powder also revealed the highest photocatalytic bleaching of MG solutions which, as in the case of UV-A light irradiation experiments, was oxidized through *N*-demethylation processes. Finally, experiments carried out using blue-light irradiation under N_2 atmosphere showed that aqueous MG solutions were not bleached by TiO_2 powders containing TPA.

1. Introduction

Since the early 1970s, when Fujishima and Honda [1] discovered that by using single crystals of rutile TiO_2 as photoelectrodes, it was possible to transform the light in chemical energy in order to generate H_2 and O_2 and Gravelle et al. found that reduced TiO_2 was able to oxidize isobutane at room temperature [2], the research about titanium dioxide (TiO_2) has increased drastically and has been extended to the area of environmental photocatalysis [3–5]. When this semiconductor is irradiated under UV light, it exhibits photocatalytic activity leading to the oxidative destruction of a wide range of organic compounds and inactivation of pathogen microorganisms on its surface. Although heterogeneous photocatalysis has shown to be a promising technology to eliminate pollutants and inactivate microorganisms in water, two important drawbacks must be overcome: (i) its overall efficiency under natural sunlight is limited to the UV-driven activity ($\lambda < 400$ nm), accounting only for ~4% of the incoming solar energy on the Earth's surface, (ii) its highest electron-hole (e^-/h^+) recombination rate [6] (around 90% of e^-/h^+ pairs are recombined in the nanosecond range). Different strategies have been proposed to overcome these problems. For instance, the increase of TiO_2 absorption and photoactivity in the visible region has attracted a lot of attention [7]. Much progress has been achieved in the field of *visible-light-active* TiO_2 by incorporation of various metallic and nonmetallic dopants into its lattice [8–12]. Recently, several authors have demonstrated that the use of N- and S-doped TiO_2 seems to be not suitable to degrade organic pollutants under visible light or solar-simulated irradiation [13–15].

On the other hand, several strategies have also been used to decrease the recombination in TiO_2 nanoparticles by adding noble metals such as silver and platinum, which have shown good results, since metals behave as electron traps [16–18].

Heteropolyoxometallates (POMs) are widely used as oxidation as well as acid catalysts [19–21]. They are also employed as effective homogeneous photocatalysts in the oxidation of organic

* Corresponding authors. Tel.: +54 221 421 1353; fax: +54 221 421 1353x125.
E-mail addresses: julianregifo@quimica.unlp.edu.ar (J.A. Rengifo-Herrera), lrpizzio@quimica.unlp.edu.ar (L.R. Pizzio).

0926-3373/$ – see front matter © 2011 Elsevier B.V. All rights reserved.
doi:10.1016/j.apcatb.2011.08.034

compounds [22] and in the degradation of organic pollutants in water [23].

The incorporation of POMs such as tungstophosphoric acid (TPA) has been explored to enhance the photocatalytic activity and the broadening of light absorption of TiO_2, obtaining good results in the destruction of organic pollutants [24,25]. In addition, it is well known that POMs could play the role of efficient photoinduced electron traps, enhancing the photocatalytic process and diminishing the e^-/h^+ recombination [26].

Herein, we report the preparation of spherical particles of TiO_2 by adding 20% and 30% (w/w) TPA via the sol–gel process and using urea as pore-forming agent. Morphological, bulk and surface features of these materials were characterized by X-ray diffraction (XRD), ^{31}P magic angle spinning-nuclear magnetic resonance (^{31}P MAS NMR), scanning electron microscopy (SEM), diffuse reflectance spectroscopy (DRS), X-ray photoelectron spectroscopy (XPS), and the pH_{pzc} was also determined. Their photocatalytic activity was tested in the bleaching of aqueous solutions of malachite green oxalate (MG), a cationic triphenyl methane dye, under UV and blue light irradiation, and compared with the values obtained using Degussa–Evonik P-25 TiO_2.

2. Experimental

2.1. Synthesis of modified TPA–TiO_2 particles

Titanium isopropoxide (Aldrich, 26.7 g) was mixed with absolute ethanol (Merck, 186.6 g) and stirred for 10 min to obtain a homogeneous solution under N_2 at room temperature, then 0.33 cm^3 of 0.28 M HCl aqueous solution was dropped slowly into the above mixture to catalyze the sol–gel reaction and was left for 3 h. Then 120 g of urea–alcohol–water (1:5:1 weight ratio) solution was added to the hydrolyzed solution under vigorous stirring, to act as template, together with an ethanol solution of $H_3PW_{12}O_{40}{\cdot}23H_2O$ (Fluka p.a.). The amount of TPA solution was fixed in order to obtain a TPA concentration of 0%, 20% and 30% by weight in the final material.

The gels were kept in a beaker at room temperature till dryness. The solids were ground into powder and extracted with distilled water for three periods of 24 h to remove urea, in a system with continuous stirring. Finally, the solids were thermally treated at 500 °C for 2 h. The samples will be named TiO_2–TPA–0%, TiO_2–TPA–20%, and TiO_2–TPA–30%, respectively.

2.2. Sample characterization

2.2.1. Scanning electron microscopy (SEM)

The secondary electron micrographs of the samples were obtained by scanning electron microscopy (SEM), using Philips Model 505 equipment, at a working potential of 15 kV, and samples coated with graphite.

2.2.2. Point of zero charge measurements

The point of zero charge (pH_{PZC}) of each sample was estimated using the mass titration method proposed by Noh and Schwarz [27]. Suspensions of the solid in deionized water ranging from 0.01% to 20% (w/w) were prepared and the pH measured after 24 h of stirring.

2.2.3. Diffuse reflectance spectroscopy (DRS)

The diffuse reflectance spectra of the materials were recorded using a UV–visible Lambda 35, Perkin–Elmer spectrophotometer, to which a diffuse reflectance chamber Labsphere RSA-PE-20 with an integrating sphere of 50 mm diameter and internal Spectralon coating is attached, in the 250–600 nm wavelength range.

2.2.4. Nuclear magnetic resonance spectroscopy (NMR)

The ^{31}P magic angle spinning-nuclear magnetic resonance (^{31}P MAS–NMR) spectra were recorded with Bruker Avance II equipment, using the CP/MAS ^{1}H–^{31}P technique. A sample holder of 4 mm diameter and 10 mm in height was employed, using 5 ms pulses, a repetition time of 4 s, and working at a frequency of 121.496 MHz for ^{31}P at room temperature. The spin rate was 8 kHz and several hundred pulse responses were collected. Phosphoric acid 85% was employed as external reference.

2.2.5. X-ray photoelectron spectroscopy (XPS)

XPS analyses were carried out with XPS Analyzer Kratos model Axis Ultra with a monochromatic AlKα and charge neutralizer. The deconvolution software program was provided by Kratos, the manufacturer of the XPS instrument.

All the binding energies were referred to the C1 s peak at 285 eV of adventitious carbon. Powder samples were prepared by deposition of the solid on carbon type stuck to the sample holder.

2.3. Photocatalytic activity under UV and blue-light irradiation

TiO_2 (1.0 g dm^{-3}; this concentration showed the best photocatalytic activity towards MG discoloration under the experimental conditions used (data not shown)) was added to a 5.0×10^{-4} M aqueous malachite green oxalate solution contained in cylindrical Pyrex bottles of 50 cm^3. Prior to UV or blue-light irradiation, the resulting suspension was kept under magnetic stirring in the dark for ca. 30 min to ensure that dye/TiO_2 surface adsorption/desorption processes were reached. The suspension was then irradiated by 5 UV black light lamps Philips TLD 18 W (emission spectra: 330–400 nm and UV intensity between 300 and 400 nm: 38 W m^{-2}) or 5 fluorescent lamps Philips TLD-18 W blue (emission spectra: 400–500 nm with UV intensity: 0.1 W m^{-2} and global intensity between 290 and 1100 nm: 60 W m^{-2}). UV and global intensity were monitored with a Kipp and Zonen (CM3) power meter (Omni instruments Ltd, Dundee, UK). The atmosphere in the cylindrical Pyrex bottle was adjusted by continuously bubbling either air or nitrogen (99.999% Carbagas, Switzerland) ensuring saturated oxygen and nitrogen conditions. Samples taken at different illumination times were filtered through membranes of 0.22 μm pore size, and the discoloration of the MG solution was followed by UV–vis spectrophotometry (Varian Cary 1-E) monitoring the absorbance at 618 nm. The initial pH of each solution was adjusted at 3.0 by adding HCl (Cl^- concentration in solution was approximately below 1 mM). The running temperature was never higher than 38 °C.

3. Results and discussion

3.1. Nanoparticle morphology, bulk and surface characterization

SEM images (Fig. 1a and b) reveal that these materials consist of spherical nanoparticles with an average diameter around 500 nm. However, when the image is magnified (insert, Fig. 1a and b), it is observed that the spherical particles are formed by the aggregation of smaller particles (see arrows). This effect is induced by urea presence. As has already been reported [28–30], urea decomposition in aqueous solution during sol–gel synthesis might produce a smooth pH increase, leading to the formation of TiO_2 nanoparticles with a controlled morphology, in this case, spherical.

In a previous work, it was found that the crystalline structure of TiO_2 nanoparticles containing TPA and annealed at 500 °C was mainly anatase. No XRD evidence of TPA, its decomposition products or WO_3 presence was found [31].

Moreover, DRS spectra (Fig. 2) showed that spherical titania nanoparticles containing TPA absorb visible light between 400 and

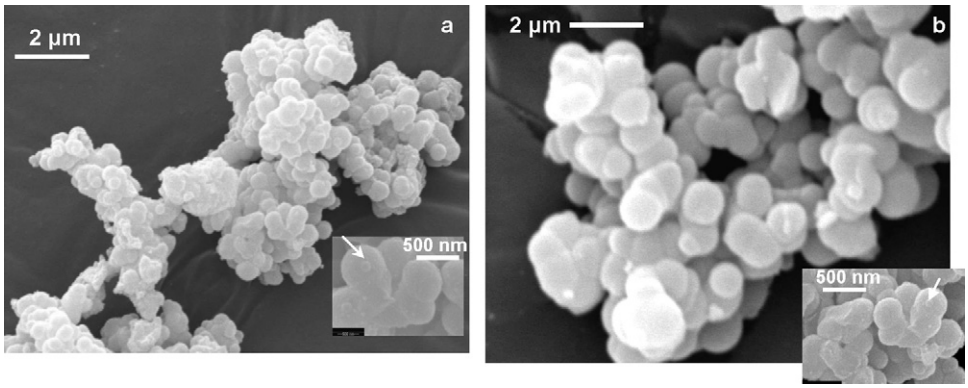

Fig. 1. SEM images of (a) TiO_2–TPA–20% and (b) TiO_2–TPA–30% powders. Inserts show magnified images and arrows reveal the presence of the smallest nanoparticles.

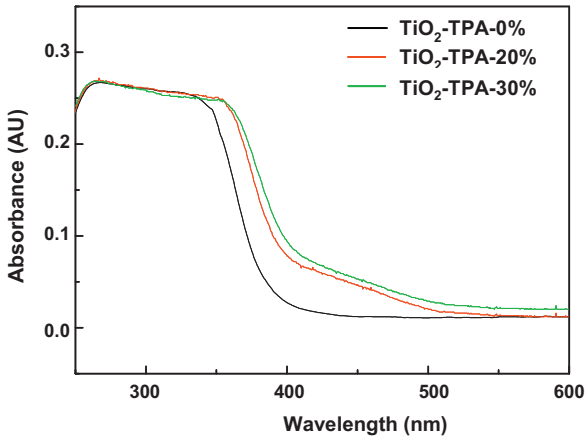

Fig. 2. DRS spectra of powders prepared with and without addition of tungstophosphoric acid.

500 nm and this visible light absorption slightly increases for higher TPA content. Table 1 shows the values of band gap energy (E_{bg}) calculated in a previous work [31] confirming the visible light absorption of the synthesized materials.

Regarding ^{31}P MAS–NMR results (Fig. 3), the presence of three lines at −14.5, −12.1, and −10.7 ppm was observed, with higher intensities when the TPA amount increases. The features are assigned to the presence of $[PW_{12}O_{40}]^{3-}$, $[P_2W_{21}O_{71}]^{6-}$ and $[PW_{11}O_{39}]^{7-}$ species [31], respectively, in both powders containing TPA. In addition, the line corresponding to $[PW_{12}O_{40}]^{3-}$ species was the most intense, revealing that in spite of the annealing step at 500 °C, an important amount of TPA remains unaltered. These results agree with the study reported by Kumbar et al. [32] where they found that TPA immobilized on titania supports remains unaltered at temperatures between 200 and 650 °C.

The generation of lacunar and dimeric species such as $[PW_{11}O_{39}]^{7-}$ and $[P_2W_{21}O_{71}]^{6-}$ could be due to pH changes because of urea decomposition occurring during the sol–gel synthesis, as has been proposed by Pope [33] through the equilibrium:

$$[PW_{12}O_{40}]^{3-} \Leftrightarrow [P_2W_{21}O_{71}]^{6-} \Leftrightarrow [PW_{11}O_{39}]^{7} \quad (1)$$

On the other hand, the presence of $[PW_{11}O_{39}]^{7-}$ leads to the generation of $[WO_4]^{2-}$ anion, through reaction 2 [33]. This reaction could occur during the sol–gel synthesis or at the annealing step.

$$[PW_{12}O_{40}]^{3-} + 6OH^- \Leftrightarrow [PW_{11}O_{39}]^{7-} + [WO_4]^{2-} + 3H_2O \quad (2)$$

In order to analyze which species are present on the material surface, XPS analysis was carried out on the samples containing 20% and 30% TPA (Fig. 4a and b, respectively). Fig. 4 shows the O1 s and Ti 2p signals for all materials. O1 s signals reveal the presence of two peaks at 530 and 532 eV due to Ti–O and Ti–OH bonds on the surface and typical of TiO_2; while the Ti 2p signals show a doublet at 459 and 465 eV corresponding to Ti^{IV} in TiO_2 [34]. However, materials containing TPA revealed the presence of W4 f and P2 p peaks. Peaks corresponding to *N* species were not found. Material synthesized in the absence of TPA showed only signals corresponding to TiO_2 (data not shown).

Table 1
pH_{pzc} and band gap energy (E_{bg}) measured for synthesized powders annealed at 500 °C.

Sample	pH_{pzc}	E_{bg} (eV)
TiO_2–TPA–0%	6.0	3.10
TiO_2–TPA–20%	4.5	2.90
TiO_2–TPA–30%	2.5	2.88

From reference [31].

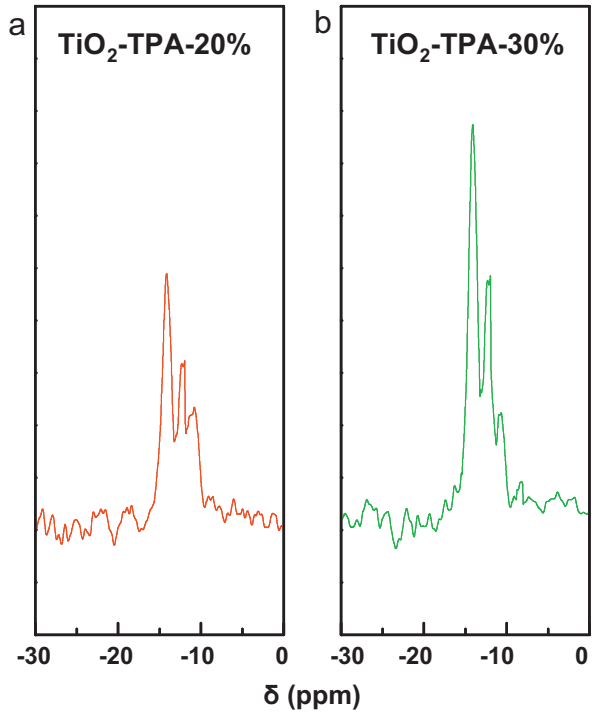

Fig. 3. ^{31}P MAS–NMR spectra of the TiO_2–TPA–20% and TiO_2–TPA–30% samples.

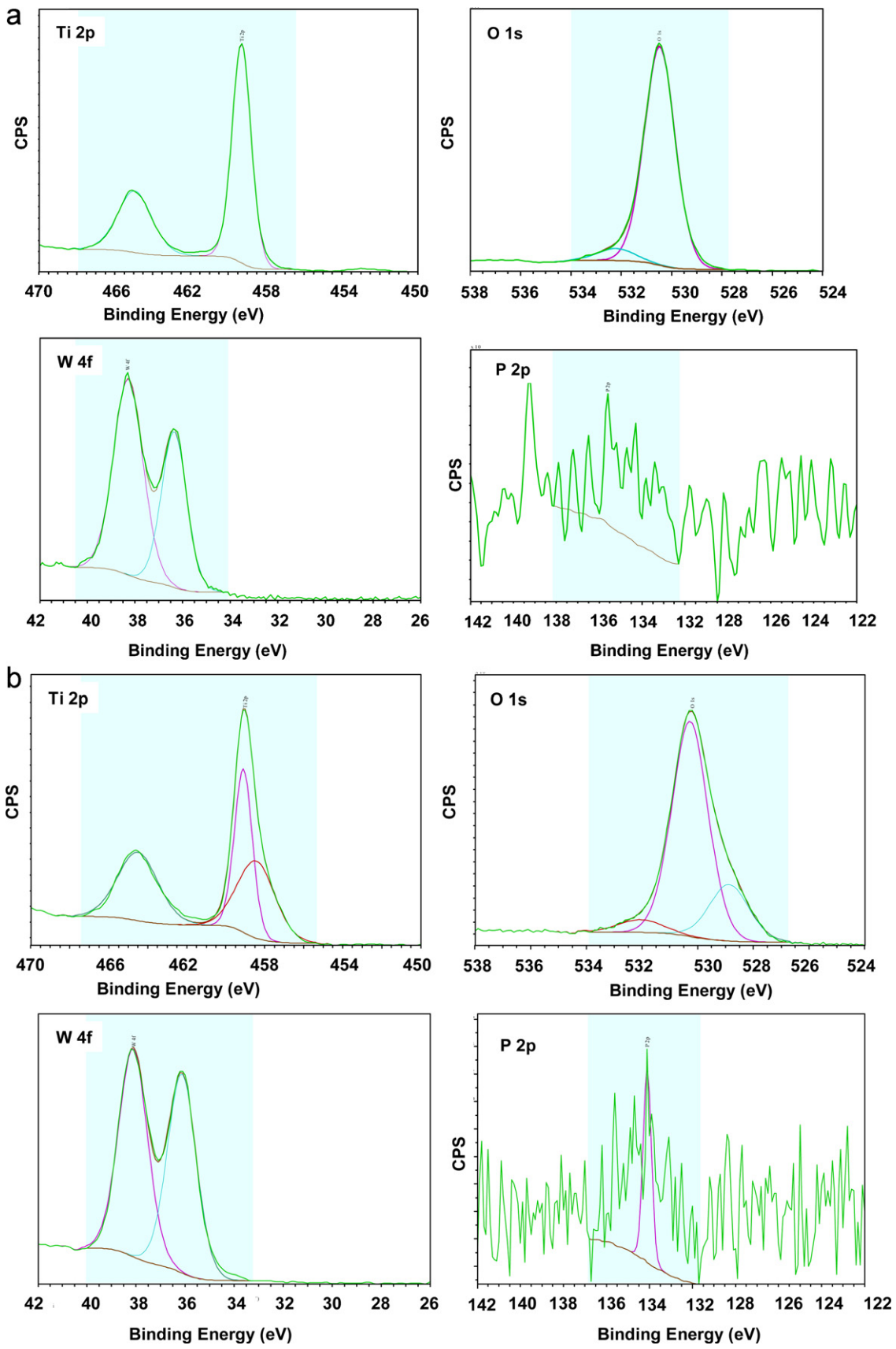

Fig. 4. XPS measurements of (a) TiO_2–TPA–20% and (b) TiO_2–TPA–30% powders.

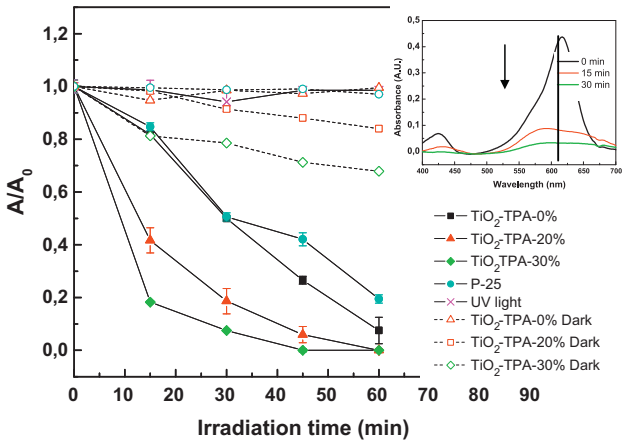

Fig. 5. Photocatalytic activity evaluated under UV light irradiation and air presence at pH 3.0 (UV intensity: 38 W m^{-2}). Insert: Spectral changes of malachite green light absorption under UV irradiation in the presence of TiO_2–TPA–30% material.

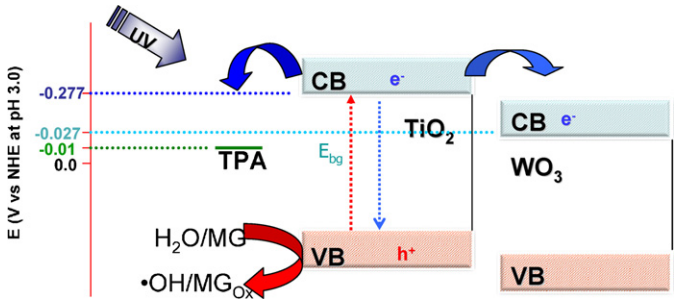

Fig. 6. Proposed scheme of the photocatalytic process occurring on TiO_2 powders containing TPA under UV light irradiation.

TPA presents a W 4f signal with a doublet at 35.8 and 37.9 eV corresponding to W (VI) [32,35]. Kumbar et al. [32] have reported that W 4f signal does not undergo any shifting when TPA is supported on TiO_2. However, for TiO_2–TPA–20% and TiO_2–TPA–30% sample, the obtained results showed that the doublet assigned to W (VI)shifts to 36.1 and 38.1 eV, respectively. These signals would be in agreement with the presence of TPA and WO_x species such as WO_3 on the TiO_2 surface [24,36–38]. Fuerte et al. [37] and Hathway et al. [38] have recently mentioned that the XPS W 4f signals often linked to presence of WO_3 in Ti-W mixed oxides could show values at 35.8 ± 0.2 eV and 36 eV respectively.

On the other hand, a weak P 2p peak due to the presence of P^{5+} was detected. It was localized at the same binding energy assigned to P^{5+} present in bulk TPA (134.2 eV) with Keggin structure [36,39]. We suggest that there is no P-doping in our samples since often XPS P 2p peaks corresponding to P-doped TiO_2 are localized at 133.0–133.5 eV [39,40].

As was mentioned above, the $[PW_{12}O_{40}]^{3-}$ decomposition can lead to the formation of $[WO_4]^{2-}$; this latter anion is often used to prepare TiO_2 containing WO_3 [35,37,41]. Thus, it can be concluded that the synthesized modified TiO_2 materials contain unaltered TPA, together with lacunar ($[PW_{11}O_{39}]^{7-}$), dimeric ($[P_2W_{21}O_{71}]^{6-}$), and WO_x species such as WO_3 (supported by ^{31}P MAS–NMR and XPS results); these latter species may be responsible for visible light absorption evidenced by DRS spectra.

On the other hand, TiO_2–TPA–30% powders showed a lower pH_{pzc} than TiO_2–TPA–20% and TiO_2–TPA–0% (Table 1). The pH_{pzc} decrease with the increment of TPA in the sample could be assigned to the presence of TPA on titania surface, whose acidic Brönsted properties are well known [21]. In addition, several authors have reported that the presence of WO_3 could also acidify the TiO_2 surface diminishing its isoelectric point [42].

3.2. Photocatalytic activity under UV-A light irradiation in the presence of molecular oxygen

Fig. 5 shows the bleaching of aqueous MG solutions in the presence or absence of TiO_2 or UV-A light at pH 3.0. UV-A light alone did not produce any bleaching effect on the malachite green solution. It is noted that black light lamps do not emit wavelengths (320 > λ < 400 nm) where the dye has its peak of maximum light absorption (λ_{max} = 617 nm) so photochemical reactions can be neglected. TPA, lacunar or dimeric species photoexcitation can also be neglected since those heteropolyoxometallates have their absorption maxima around 265 nm [19,21].

Experiments carried out in the absence of light revealed a high dye adsorption on the TiO_2–TPA–30% sample, as shown in Fig. 5. This could be due to the fact that this material has a pH_{pzc} around 2.5 (Table 1) and, under the experimental conditions (initial solution pH at 3.0), titania surface would be partially negatively charged. MG is a cationic dye under these pH conditions, thus its adsorption on TiO_2 surfaces would be favored. On the other hand, the presence of unaltered $[PW_{12}O_{40}]^{3-}$ on titania surface could also be responsible for this adsorption. MG dye has $-N(CH_3)_2$ groups with basic properties, thus acid–base interactions between malachite green and TPA could also be responsible for this enhanced adsorption.

However, when UV-A light was turned on, the aqueous dye solution underwent a photocatalytic bleaching. This process was faster in the presence of TiO_2–TPA–30% powder than with TiO_2–TPA–20% or TiO_2–TPA–0% powders, and even faster than with Degussa–Evonik P-25 (Fig. 5).

The insert in Fig. 5 shows the spectral changes on the UV–vis absorption spectrum of aqueous MG solution during the photocatalytic process when the TiO_2–TPA–30% sample was used. The main absorption peak at 618 nm underwent a blue shift due to oxidative processes of *N*-demethylation of the dye, as has already been reported in a previous paper using Degussa–Evonik P-25 TiO_2 powder as photocatalyst [43].

Taking into account these results, a possible mechanism of the photocatalytic activity of TiO_2 powders containing TPA under UV-A irradiation can be suggested (Fig. 6).

When charge separation is generated by UV-A irradiation, most of the electrons promoted to the TiO_2 conduction band are recombined. However, the presence of unaltered TPA in the materials could play an important role, since it is well known that this heteropolycompound is an efficient electron trap [21]. The first reduction potential of TPA is around −0.01 V (vs. NHE) [21], while the TiO_2 conduction band potential at pH 3.0 is −0.277 V (vs. NHE) [4], so the photoinduced electron transfer from TiO_2 to TPA seems to be thermodynamically favored. Thus, recombination of e^-/h^+ would be diminished and this fact would explain why the TiO_2–TPA–30% and TiO_2–TPA–20% powders showed a higher photocatalytic activity than Degussa–Evonik P-25.

On the other hand, the presence of WO_x species, such as WO_3, could also decrease the recombination since the redox potential of the WO_3 conduction band (−0.027 V vs. NHE at pH 3.0) is more positive than that of TiO_2 [24,40,44–47], thus electron transfer induced by UV-A light absorption from TiO_2 to WO_3 would also be thermodynamically allowed.

In addition, the highest MG adsorption on the surface of the TiO_2–TPA–30% sample (Fig. 5) could also benefit the photocatalytic activity since dye molecules will be closer to the titania surface, easily allowing its oxidative degradation by valence band holes or surface bonded •OH radicals.

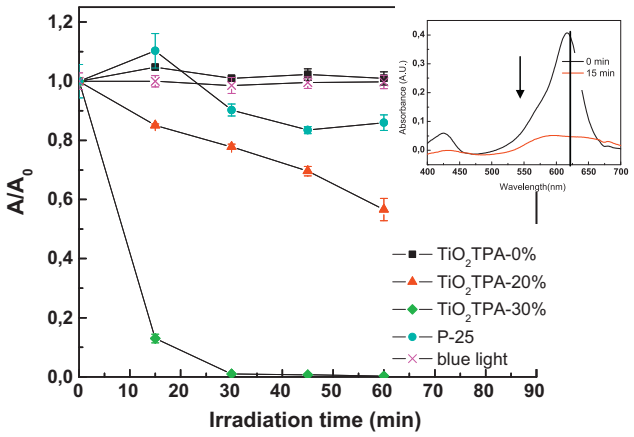

Fig. 7. Photocatalytic activity evaluated under blue-light irradiation and air presence at pH 3.0 (global intensity between 290 and 1100 nm: 60 W m^{-2}, UV intensity: 0.1 W m^{-2}). Insert: Spectral changes of malachite green light absorption under blue-light irradiation in the presence of TiO_2–TPA–30% material.

3.3. *Photocatalytic activity under blue-light irradiation in the presence and absence of molecular oxygen*

According to the emission spectrum of blue lamps ($400 > \lambda < 500$ nm) used during these experiments, photochemical or photosensitized reactions affecting the color of aqueous dye solutions can be neglected, since these lamps do not emit light in wavelengths where MG could strongly absorb light.

In the presence of oxygen from the air (Fig. 7), the aqueous MG solution was rapidly bleached (100% bleaching at 30 min) when the TiO_2–TPA–30% sample was added and the suspension was exposed to blue light at pH 3.0. On the other hand, after 30 min of irradiation in the same conditions, the samples TiO_2–TPA–20%, TiO_2–TPA–0%, and TiO_2 Degussa–Evonik P-25 showed a bleaching of 20%, 10% and 0%, respectively.

Regarding the UV–vis spectra of aqueous malachite green solution during the photocatalytic reaction using TiO_2–TPA–30% powder (insert, Fig. 7), evidence of the *N*-demethylation process responsible for the bleaching of the solution was also found, because a blue shift of its main absorption peak at 618 nm takes place.

Additionally, when experiments were carried out in the absence of molecular oxygen by continuous N_2 bubbling, the samples did not show any photocatalytic activity (data not shown).

These results provide evidence that species responsible for visible light absorption could also play an important role in MG photocatalytic bleaching. In Section 3.1, it was suggested that WO_x species would be responsible for visible light absorption. Among these species, it is possible that WO_3 coupled with TiO_2 could be present, as has been mentioned by other authors [24,41,42]. WO_3 is a semiconductor with lower band gap energy (E_{bg}: 2.8 eV) and more cathodic band positions than the TiO_2 conduction band [40]. Species such as WO_3 could absorb blue light, producing charge separation. Holes produced in the WO_3 valence band are oxidative enough to degrade adsorbed MG molecules directly or via •OH radicals. On the other hand, since the conduction band of WO_3 is more cathodic [44], the molecular oxygen reduction by photoinduced e^-_{CB} could not be thermodynamically favored. However, TPA present on titania could act as electron trap benefiting the charge separation. Then reduced TPA could be oxidized by molecular oxygen yielding the superoxide radical ($\bullet O_2^-$) (Fig. 8).

Although in a recent study, we reported that aqueous MG solutions could be photocatalytically bleached through reductive reactions leading to the generation of a colorless substance called leuco malachite green (LMG) by UV-illuminated Degussa–Evonik P-25 nanoparticles in the absence of oxygen and at pH 3.0 [43], this phenomenon was not observed when the TiO_2–TPA–30% powder was illuminated with visible light in the absence of molecular oxygen. It is suggested that when TPA (first redox potential −0.01 V vs. NHE) is reduced by blue-light photoinduced conduction band electrons in WO_x species such as WO_3 (whose CB redox potential of electrons at pH 3.0 is around −0.027 V vs. NHE), these reduced species would not be able to inject an electron to dye molecules (Fig. 8). Besides, reduced tungstophosphoric acid (TPA^-) on titania surface requires the presence of molecular oxygen to regenerate the TPA in order to keep its property of photoinduced electron trapping and avoid the charge carrier recombination.

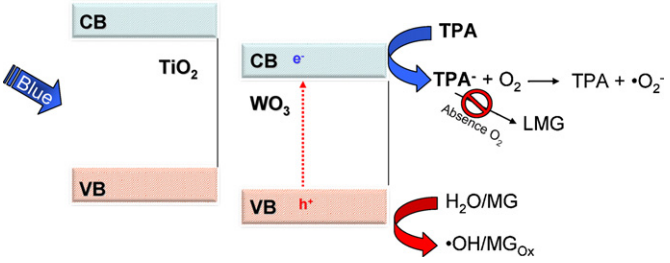

Fig. 8. Proposed scheme of the photocatalytic process occurring on TiO_2 powders containing TPA under visible light irradiation.

4. Conclusions

Spherical TPA modified anatase TiO_2 nanoparticles were successfully prepared through the sol–gel process, and annealed at 500 °C. These materials showed visible light absorption due to a partial decomposition of TPA, leading probably to the formation of visible light-absorbing WO_x species such as WO_3. However, a high proportion of TPA remained unaltered even after the annealing step. The TiO_2–TPA–30% sample showed the lowest pH_{pzc}, mainly due to the presence of TPA and/or WO_x species on the titania surface.

Regarding the photocatalytic activity of the synthesized powders, TiO_2–TPA–30% material gave evidence of the highest photocatalytic activity towards the bleaching of aqueous MG solutions under UV and blue-light irradiation. This dye underwent an oxidative *N*-demethylation process induced either by UV or blue light-irradiated TiO_2–TPA powders in the presence of molecular oxygen from the air.

The photocatalytic activity of TiO_2–TPA–30% and TiO_2–TPA–20% samples was higher than that of Degussa–Evonik P-25 TiO_2 under both UV and blue-light irradiation.

In the absence of molecular oxygen by continuous N_2 bubbling, and under blue-light irradiation, aqueous dye solutions did not undergo any bleaching effect.

It is suggested that under UV light irradiation, anatase TiO_2 particles contained in TiO_2–TPA–30% powders are excited, thus inducing charge separation. However, the presence of TPA or WO_x species would benefit the photocatalytic process since these species could act as traps for the photoinduced electrons, diminishing the recombination.

Under blue-light irradiation, WO_x species such as WO_3 could be responsible for the photocatalytic activity observed, producing charge separation. Since WO_3 band positions are more cathodic than those of TiO_2, molecular oxygen reduction could not be expected; however, the presence of TPA could overcome this problem, since it could act as a photoinduced electron trap. Thus photoinduced holes on WO_x species could oxidize the adsorbed malachite green molecules directly or via •OH radical formation under blue-light irradiation.

Acknowledgements

The authors thank the Cooperation@EPFL for its support to the Argentinean-Swiss cooperation project and to CONICET for the support to the project PIP 1938 and the post-doctoral fellow granted to J.A. Rengifo-Herrera. J.A. Rengifo-Herrera thanks the support and collaboration of Dr. Cesar Pulgarin and Dr. Christophe Roussel (EPFL-Switzerland). We thank specially Aurélie Demierre for her collaboration in the laboratory.

References

[1] A. Fujishima, K. Honda, Nature 238 (1972) 37–38.
[2] P.C. Gravelle, P.C. Juillet, F. Meriaudeau, S.J. Teichner, Disc. Faraday Soc. 52 (1971) 140–148.
[3] P. Pichat, Water Sci. Technol. 55 (2007) 167–173.
[4] A. Fujishima, X. Zhang, D.A. Tryk, Surf. Sci. Rep. 68 (2008) 515–582.
[5] S. Kwon, M. Fan, A.T. Cooper, H. Yang, Crit. Rev. Environ. Sci. Technol. 38 (2008) 197–226.
[6] T. Berger, M. Sterrer, O. Diwald, E. Knozinger, D. Panayotov, T.L. Thompson, J.T. Yates, J. Phys. Chem. B 109 (2005) 6061–6068.
[7] D. Mitoraj, H. Kisch, Sol. State Phenom. 162 (2010) 49–75.
[8] M. Anpo, M. Takeuchi, J. Catal. 216 (2003) 505–516.
[9] E.A. Reyes-García, Y. Sun, D. Raftery, J. Phys. Chem. C 111 (2007) 17146–17154.
[10] M. Katoh, H. Aihara, T. Horikawa, T. Tomida, J. Colloid Interface Sci. 298 (2006) 805–809.
[11] C. Di Valentin, E. Finazzi, G. Pacchioni, A. Selloni, S. Livraghi, M.C. Paganini, E. Giamello, Chem. Phys. 339 (2007) 44–56.
[12] J.A. Rengifo-Herrera, K. Pierzchala, A. Sienkiewicz, L. Forro, J. Kiwi, J.-E. Moser, C. Pulgarin, J. Phys. Chem. C 114 (2010) 2717–2723.
[13] M. Mrowetz, W. Bakerski, A.J. Colussi, M.R. Hoffmann, J. Phys. Chem. B 108 (2004) 17269–17273.
[14] J.A. Rengifo-Herrera, C. Pulgarin, Sol. Energy 84 (2010) 37–43.
[15] T. Ohno, Z. Miyamoto, K. Nishijima, H. Kanemitsu, X.Y. Feng, Appl. Catal. A Gen. 309 (2006) 155–156.
[16] P. Pichat, R. Enriquez, E. Mietton, Sol. State. Phenom. 162 (2010) 41–48.
[17] C.A. Emilio, M.I. Litter, M. Kunst, M. Bouchard, C. Colbeau-Justin, Langmuir 22 (2006) 3606–3613.
[18] V. Iliev, D. Tomova, L. Bilyarska, A. Eliyas, L. Petrov, Appl. Catal. B Environ. 63 (2006) 266–271.
[19] T. Okuhara, N. Mizuno, M. Misono, Adv. Catal. 41 (1996) 113–252.
[20] L.R. Pizzio, P.G. Vázquez, C.V. Cáceres, M.N. Blanco, Appl. Catal. A Gen. 256 (2003) 125–129.
[21] E. Papaconstantinou, Chem. Soc. Rev. 18 (1989) 1–31.
[22] A. Mylonas, E. Papaconstantinou, J. Mol. Catal. A Chem. 92 (1994) 261–267.
[23] J. Ryu, W. Choi, Environ. Sci. Technol. 38 (2004) 2928–2933.
[24] V. Fuchs, L. Méndez, M. Blanco, L. Pizzio, Appl. Catal. A Gen. 358 (2009) 73–78.
[25] C. Yu, J.C. Yu, W. Zhou, K. Yang, Catal. Lett. 140 (2010) 172–183.
[26] P. Ngaotrakanwiwat, S. Saitoh, Y. Ohko, T. Tatsuma, A. Fujishima, J. Electrochem. Soc. 150 (2003) A1405–A1407.
[27] J.S. Noh, J.A. Schwarz, J. Colloid Interface Sci. 114 (1988) 433–439.
[28] G.J. Soler-Illia, M. Jobaggy, R.J. Candal, A.E. Regazzoni, M.A. Blesa, J. Disp. Sci. Technol. 19 (1998) 207–228.
[29] G.J. Soler-Illia, R.J. Candal, A.E. Regazzoni, M.A. Blesa, Chem. Mater. 9 (1997) 184–191.
[30] M. Zhou, J. Yu, H. Yu, J. Mol. Catal. A Chem. 313 (2009) 107–113.
[31] V.M. Fuchs, E.L. Soto, M.N. Blanco, L.R. Pizzio, J. Colloid Interface Sci. 327 (2008) 403–411.
[32] S.M. Kumbar, G.V. Shanbhag, F. Lefebvre, S.B. Halligudi, J. Mol. Catal. A Chem. 256 (2003) 324–334.
[33] M.T. Pope, Heteropoly and Isopoly Oxometalates, Springer, Berlin, 1983.
[34] L.-Q. Wang, D.R. Baer, M.H. Engelhard, Surf. Sci. 320 (1994) 295–306.
[35] P.A. Jalil, M. Faiz, N. Tabet, N.M. Hamdan, Z. Hussain, J. Catal. 217 (2003) 292–297.
[36] X.-L. Yang, W.-L. Dai, C. Guo, H. Chen, Y. Cao, H. Li, H. He, K. Fan, J. Catal. 234 (2005) 438–450.
[37] A. Fuerte, M.D. Hernández-Alonso, A.J. Maira, A. Martinez-Arias, M. Fernandez-Garcia, J.C. Conesa, J. Soria, G. Munuera, J. Catal. 212 (2002) 1–9.
[38] T. Hathway, E.M. Rockafellow, Y.-C. Oh, W.S. Jenks, J. Photochem. Photobiol. A Chem. 207 (2009) 197–203.
[39] L. Lin, R.Y. Zheng, J.L. Xie, Y.X. Zhu, Y.C. Xie, Appl. Catal. B Environ. 76 (2007) 196–202.
[40] Y. Zhang, W. Fu, H. Yang, S. Liu, P. Sun, M. Yuan, D. Ma, W. Zhao, Y. Sui, M. Li, Y. Li, Thin Solid Films 518 (2009) 99–103.
[41] O. Lorret, D. Francova, G. Waldner, N. Stelzer, Appl. Catal. B: Environ. 91 (2009) 39–46.
[42] N. Couselo, F.S. Garcia-Einschlag, R.J. Candal, M. Jobbagy, J. Phys. Chem. C 112 (2008) 1094–1100.
[43] J.A. Rengifo-Herrera, M.N. Blanco, L.R. Pizzio, C. Roussel, C. Pulgarin, Photochem. Photobiol. Sci. 10 (2011) 29–34.
[44] M.T. Nenadovic, T. Rajh, O.I. Micic, A.J. Nozik, J. Phys. Chem. 88 (1984) 5827–5830.
[45] X.Z. Li, F.B. Li, C.L. Yang, W.K. Ge, J. Photochem. Photobiol. A Chem. 141 (2001) 209–217.
[46] R. Bathe, P.S. Patil, Sol. Energ. Mat. Sol. C 91 (2007) 1097–1101.
[47] A.K.L. Sajjad, S. Shamaila, B. Tian, F. Chen, J. Zhang, Appl. Catal. B Environ. 91 (2009) 397–405.